Molecular Cell, Vol. 7, 461–473, March, 2001, Copyright ©2001 by Cell Press

dpl-1 DP and *efl-1* E2F Act with *lin-35* Rb to Antagonize Ras Signaling in *C. elegans* Vulval Development

Craig J. Ceol and H. Robert Horvitz*
Howard Hughes Medical Institute
Department of Biology
Massachusetts Institute of Technology
Cambridge, Massachusetts 02139

Summary

The synthetic multivulva (synMuv) genes define two functionally redundant pathways that antagonize RTK/Ras signaling during *Caenorhabditis elegans* vulval induction. The synMuv gene *lin-35* encodes a protein similar to the mammalian tumor suppressor pRB and has been proposed to act as a transcriptional repressor. Studies using mammalian cells have shown that pRB can prevent cell cycle progression by inhibiting DP/E2F-mediated transcriptional activation. We identified *C. elegans* genes that encode proteins similar to DP or E2F. Loss-of-function mutations in two of these genes, *dpl-1* DP and *efl-1* E2F, caused the same vulval abnormalities as do *lin-35* Rb loss-of-function mutations. We propose that rather than being inhibited by *lin-35* Rb, *dpl-1* DP and *efl-1* E2F act with *lin-35* Rb in transcriptional repression to antagonize RTK/Ras signaling during vulval development.

Introduction

Signal transduction pathways can control the specification of cell fates during metazoan development. Some of the pathways used for cell fate specification also act in tumorigenesis in mammals (Potter et al., 2000). Such signal transduction pathways include both protooncogenes and tumor suppressor genes.

Counterparts of mammalian protooncogenes and tumor suppressor genes play opposing roles in the determination of cell fates during the development of the hermaphrodite vulva of the nematode *Caenorhabditis elegans*. A receptor tyrosine kinase (RTK)- and Ras-mediated signal transduction pathway induces the development of the vulva (Ferguson et al., 1987; reviewed by Sternberg and Han, 1998). During the second larval stage of *C. elegans* development, a set of six ectodermal blast cells, P(3–8).p, are present along the ventral midline. Each of these six cells has the capacity to adopt either 1° or 2° vulval cell fates or a 3° nonvulval cell fate. In the wild type, P(5–7).p are induced by a signal from the neighboring gonadal anchor cell to adopt vulval fates, and these cells divide to together generate the 22 descendants that make up the adult vulva. P3.p, P4.p, and P8.p are not induced and adopt a nonvulval fate, dividing once and fusing with the syncytial hypodermis. The anchor cell signal activates an RTK/Ras pathway in P(5–7).p. Mutations that reduce RTK/Ras pathway activity, including loss-of-function mutations in *let-23* RTK or *let-60* Ras, cause P(5–7).p to adopt nonvulval fates, resulting in a vulvaless (Vul) phenotype. By contrast, mutations that increase RTK/Ras pathway activity, such as gain-of-function mutations in *let-60* Ras, cause P3.p, P4.p, and P8.p to ectopically adopt vulval fates, resulting in a multivulva (Muv) phenotype.

The activity of the RTK/Ras pathway is antagonized by the synthetic multivulva (synMuv) genes (Horvitz and Sulston, 1980; Ferguson and Horvitz, 1989). On the basis of genetic interactions, the synMuv genes have been grouped into two classes, A and B. Animals with loss-of-function mutations in a class A and a class B gene are Muv, whereas animals mutant in a single gene or genes of a single class are non-Muv. Mutations identifying 5 class A and 17 class B genes have been isolated (Horvitz and Sulston, 1980; Ferguson and Horvitz, 1989; Hsieh et al., 1999; Solari and Ahringer, 2000; von Zelewsky et al., 2000) (H. R. H., C. J. C., X. Lu, and P. Sternberg, unpublished results). Classes A and B are proposed to define functionally redundant pathways that negatively regulate vulval induction (Ferguson and Horvitz, 1989).

A molecular mechanism by which some of the class B synMuv genes act was revealed by the finding that the class B gene *lin-35* encodes a protein similar to the mammalian tumor suppressor pRB (Lu and Horvitz, 1998). Among other functions, pRB and the related proteins p107 and p130 bind to and modulate the activities of DP/E2F heterodimeric transcription factors (reviewed by Dyson, 1998; Lavia and Jansen-Durr, 1999). DP/E2F heterodimers are proposed to be regulators of the G1-to-S phase transition of the cell cycle. "Free" DP/E2F heterodimers that are not bound by pRB, p107, or p130 activate the transcription of genes required for S phase. However, when associated with DP/E2F heterodimers, pRB family proteins are thought to repress DP/E2F-regulated genes, thereby inhibiting premature expression of genes required for S phase and preventing inappropriate S phase entry. pRB can recruit proteins involved in chromatin modification and transcriptional repression, including the histone deacetylase HDAC1, to promoters containing DP/E2F binding sites (Brehm et al., 1998; Luo et al., 1998; Magnaghi-Jaulin et al., 1998). This latter function appears to be conserved in *C. elegans*, as two genes with class B synMuv activity, *hda-1* and *lin-53*, encode proteins similar to the class I histone deacetylase HDAC1 and the histone deacetylase-associated protein RbAp48, respectively (Lu and Horvitz, 1998). Based on these findings, the class B synMuv genes are proposed to repress the transcription of genes required for vulval cell fate specification.

Here we report the identification and characterization of *C. elegans* genes encoding DP and E2F family members. *dpl-1* (*dpl*, DP-like) and *efl-1* (*efl*, E2F-like) are class B synMuv genes that act with *lin-35* Rb to negatively regulate vulval induction, thereby antagonizing *let-23* RTK/*let-60* Ras signaling.

*To whom correspondence should be addressed (e-mail: horvitz@mit.edu).

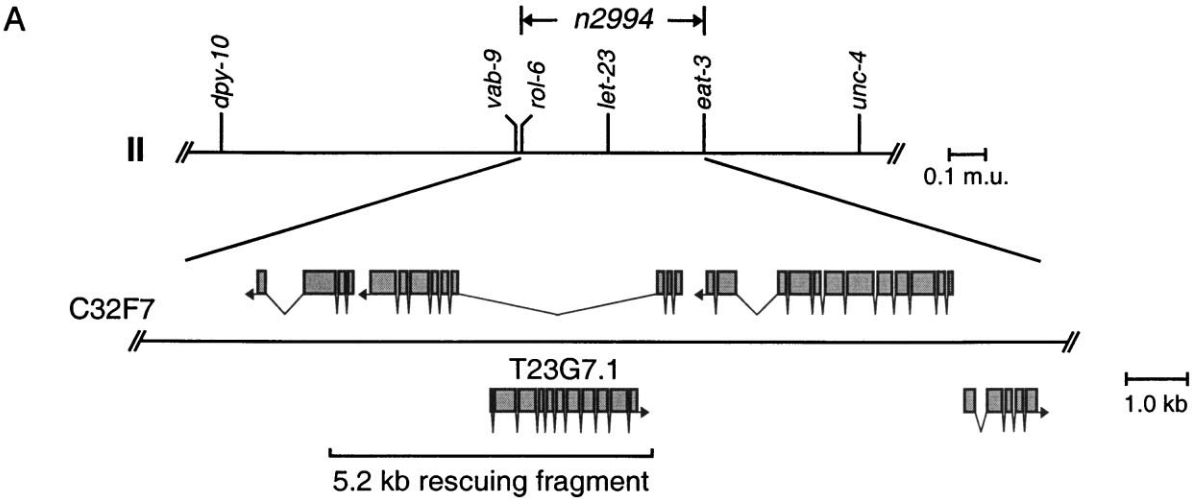
A
n2994
dpy-10
vab-9
rol-6
let-23
eat-3
unc-4
II
0.1 m.u.
C32F7
T23G7.1
1.0 kb
5.2 kb rescuing fragment

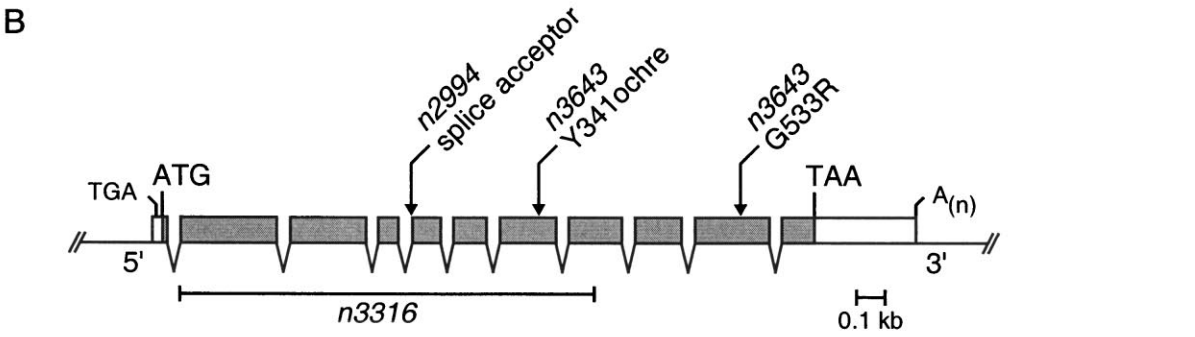
B
n2994
splice acceptor
n3643
Y341ochre
n3643
G533R
TGA
ATG
TAA
A(n)
5'
3'
n3316
0.1 kb

C


n3316 DELETION
DPL-1
Hs DP-1
Hs DP-2
dDP
DNA-BINDING
n2994 SPLICE
E2F-BINDING
n3643 Y341STOP
n3316 DELETION
n3643 G533R

Results

The Class B synMuv Mutation *n2994* Affects a DP-Related Gene

The class B synMuv mutation *n2994* was isolated in a screen for synMuv mutants and was mapped using deficiencies to a region of LGII between the cloned genes *rol-6* and *eat-3* (J. Thomas and H. R. H., unpublished results). We injected genomic DNA clones (Mello et al., 1991) from this region into *n2994*; *lin-15A(n433)* mutants to obtain transformation rescue. (*lin-15* is a complex locus of two genes, *lin-15A* and *lin-15B*, which encode class A synMuv and class B synMuv genes, respectively.) (Clark et al., 1994; Huang et al., 1994). The Muv phenotype was rescued both by the cosmid C32F7 and by a 5.2 kb PvuII-PvuII subclone of C32F7 (Figure 1A). The DNA sequence of this subclone contains one complete predicted gene, T23G7.1, which encodes a protein similar to human DP-1 and other DP family proteins (*C. elegans* Sequencing Consortium, 1998). We named this gene *dpl-1* (*dpl*, DP-like). We obtained *dpl-1* cDNA clones (see supplemental experimental procedures at www.molecule.org/cgi/content/full/7/3/461/DC1), the longest of which contains a single open reading frame that encodes a protein of 598 amino acids. An in-frame stop codon precedes the putative initiator methionine codon, suggesting that this open reading frame is full length. We determined the sequence of *dpl-1* in *n2994* mutants and found a splice-acceptor mutation preceding the fifth exon (Figures 1B and 1C). We isolated another *dpl-1* allele, *n3643*, in a screen for synMuv mutants (C. J. C and H. R. H., unpublished results) and found two alterations in the *dpl-1* locus: a nonsense mutation predicted to truncate the DPL-1 protein after 340 amino acids and a missense mutation 192 residues downstream of the nonsense mutation (Figures 1B and 1C). The gene affected by *n2994* was previously known as *lin-55* (Lu and Horvitz, 1998).

The DPL-1 protein shares extensive sequence similarity with DP family proteins, particularly in domains required by DP-1 for dimerization with E2F-1 and for enhanced DNA binding of the resultant DP-1/E2F-1 complex (Figure 1C; Girling et al., 1993; Helin et al., 1993). DPL-1 is the only DP family member predicted by the nearly complete *C. elegans* genome sequence (*C. elegans* Sequencing Consortium, 1998).

A *dpl-1* DP Null Allele Causes a synMuv Phenotype

Mammalian DP proteins participate both in transcriptional activation and, by targeting pRB-family proteins to promoters, in transcriptional repression (reviewed by Lavia and Jansen-Durr, 1999). Given the potential dual activation and repression functions of DPL-1, we sought to determine if the synMuv phenotype caused by *dpl-1 (n2994)*, which is similar to the phenotype caused by *lin-35* Rb loss-of-function mutations, was caused by a gain of *dpl-1* function, suggesting antagonism by *lin-35* Rb, or was caused by a loss of *dpl-1* function, indicating *dpl-1* action with *lin-35* Rb.

Gene dosage experiments indicate that *n2994* causes a loss rather than a gain of *dpl-1* function. Specifically, *dpl-1(n2994)/+; lin-15A(n433)* animals are non-Muv, whereas *dpl-1(n2994)/mnDf67; lin-15A(n433)* mutants, like *dpl-1(n2994); lin-15A(n433)* mutants, have a highly penetrant Muv phenotype (Table 1). *mnDf67* is a deficiency that removes the *dpl-1* locus (J. Thomas and H. R. H., unpublished results).

To confirm these findings and to study further the consequences of a *dpl-1* loss of function, we isolated the *dpl-1* deletion allele *n3316* (see supplemental experimental procedures at www.molecule.org/cgi/content/full/7/3/461/DC1). *n3316* removes 1421 base pairs of the *dpl-1* locus, deleting exons that encode the conserved DPL-1 DNA binding and dimerization domains (Figure 1B). The predicted DPL-1 protein in *n3316* mutants contains the first three amino acids of DPL-1 followed by four unrelated amino acids prior to truncation.

dpl-1(n3316) caused a Muv phenotype in a class A synMuv background but not in a class B synMuv background (Table 1), confirming that *dpl-1* is a class B synMuv gene. In addition, *dpl-1(n3316)* caused hermaphrodite sterility as a consequence of defects in ovulation and, in *trans* to partial loss-of-function *dpl-1* alleles, caused embryonic lethality (C. J. C. and H. R. H., unpublished results). The severe effect of the *n3316* deletion on the *dpl-1* locus combined with our observation that *dpl-1(n3316)* behaves genetically like the deficiency *mnDf67* (in heterozygotes with the *dpl-1(n2994)* and *dpl-1(n3316)* alleles) for the synMuv and sterile phenotypes indicates that *n3316* is a null allele of *dpl-1* (Table 1; C. J. C. and H. R. H., unpublished observations).

DPL-1 Is Broadly Expressed and Is Localized to Nuclei

We obtained a crude rabbit polyclonal antiserum raised against DPL-1 (kindly provided by B. Page and J. Priess; Page et al., 2001 [this issue of *Molecular Cell*]). We purified these antibodies against a carboxy-terminal fragment of DPL-1 (see Experimental Procedures) predicted to be truncated by the *dpl-1(n3643)* premature stop co-

Figure 1. *dpl-1* Cloning

(A) The top panel shows the genetic map location of the class B synMuv allele *n2994* on linkage group II. The bottom panel shows a segment of the rescuing cosmid C32F7 containing the *dpl-1* gene and other predicted genes. Arrows indicate the direction of transcription. The PvuII-PvuII subclone derived from C32F7 that rescues the Muv phenotype of *n2994; lin-15A(n433)* mutants is indicated.

(B) Gene structure of *dpl-1* as derived from cDNA and genomic sequences. Coding sequences are shaded. Translation initiation and termination codons and the poly(A) tail are indicated. An in-frame stop codon upstream of the translation initiation codon is also shown. The positions of and changes caused by *dpl-1* point mutations are indicated above (arrows), and the sequence deleted in the *n3316* mutant is indicated below (bracket). *n3643* has two point mutations, one causing a tyrosine-to-ochre substitution and the other a glycine-to-arginine substitution.

(C) Alignment of DPL-1 with human DP-1 (GenBank accession number NP_009042), human DP-2 (Q14188) and *Drosophila* DP (B55745). Solid boxes indicate identities with DPL-1. Arrowheads indicate the site of the splice junction affected by *n2994* and the sites of the two *n3643* mutations. The sequence removed by *n3316* is indicated by brackets. The DNA binding and E2F binding domains of human DP-1 are underlined with solid and hatched lines, respectively (Girling et al., 1993; Wu et al., 1995).

Table 1. *dpl-1* and *efl-1* Mutations Cause a synMuv Phenotype

Genotype	Percent Muv (n)
N2	0 (221)
lin-15A(n433)	0 (143)
lin-15A(n767)	0 (155)
lin-15B(n744)	0 (108)
dpl-1(n2994)	0.6 (173)
dpl-1(n3316)	0 (112)
dpl-1(n3643)	0 (132)
dpl-1(RNAi)	0 (102)
dpl-1(n3316 RNAi)	1.6 (123)
efl-1(n3318)	0 (202)
efl-1(n3639)	0 (84)
mnDf67/+	0 (116)
dpl-1(n2994)/+	0 (167)
dpl-1(n3316)/+	0 (126)
dpl-1(n2994)/dpl-1(n3316)	0 (101)
dpl-1(n2994)/mnDf67	0 (101)
dpl-1(n3316)/mnDf67	0 (113)
dpl-1(n2994); lin-15A(n433)	100 (366)
dpl-1(n3316); lin-15A(n433)	99 (103)
dpl-1(n3316); lin-15B(n744)	0 (150)
dpl-1(n3643); lin-15A(n433)	81 (229)
mnDf67/+; lin-15A(n433)	0 (221)
dpl-1(n2994)/+; lin-15A(n433)	0 (170)
dpl-1(n3316)/+; lin-15A(n433)	0 (105)
dpl-1(n2994)/dpl-1(n3316); lin-15A(n433)	99 (127)
dpl-1(n2994)/mnDf67; lin-15A(n433)	99 (200)
dpl-1(n3316)/mnDf67; lin-15A(n433)	98 (102)
lin-38(n751); efl-1(n3318)	100 (129)
efl-1(n3318); lin-15A(n433)	88 (193)
efl-1(n3318); lin-15A(n767)	100 (112)
efl-1(n3318); lin-15B(n744)	1 (176)
efl-1(n3318); efl-2(RNAi)	0 (214)
efl-1(n3318); lin-15A(n433); efl-2(RNAi)	84 (238)
efl-1(n3639); lin-15A(n767)	100 (51)

To analyze the Muv phenotype of *dpl-1* mutants, L4 larvae were scored for the presence of pseudovulval invaginations using Nomarski DIC optics. The complete genotypes of animals scored in either *lin-15A(+)* or *lin-15A(n433)* backgrounds were, from top to bottom, as follows: *dpl-1(n2994)*, *dpy-10(e128) dpl-1(n3316) +/+ dpl-1 (n3316) unc-4(e120)*, *dpl-1(n3643)*, *dpl-1(RNAi)*, *+mnDf67 unc-4 (e120)/dpy-10(e128) ++*, *dpy-10(e128) dpl-1(n2994)/++*, *+dpl-1 (n3316) unc-4(e120)/dpy-10(e128) ++*, *dpy-10(e128) dpl-1(n2994) +/+ dpl-1(n3316) unc-4(e120)*, *dpy-10(e128) dpl-1(n2994) +/+ mnDf67 unc-4(e120)*, *dpy-10(e128) dpl-1(n3316) +/+ mnDf67 unc-4 (e120)*. To analyze the Muv phenotype of *efl-1(n3318)* and *efl-1 (n3639)* homozygotes in the specified genetic backgrounds, we scored L4 Unc progeny from *+ unc-76(e911) efl-1(n3318) +/rol-4(sc8) ++ dpy-21(e428)* and from *+ efl-1(n3639) +/rol-4(sc8) + dpy-21(e428)* mothers, respectively, for the presence of pseudovulval invaginations using Nomarski DIC optics. Animals were recovered from microsope slides and scored for the Ste Mel and Ste phenotypes to confirm the presence of *efl-1(n3318)* and *efl-1(n3639)*, respectively. To analyze interaction between *efl-1* and *efl-2 + unc-76(e911) efl-1(n3318) +/rol-4(sc8) ++ dpy-21 (e428)*; *lin-15(n433)* mothers were injected with *efl-2* RNA, and their progeny were scored as described above.

don. The purified antibodies recognized a single band of about 70 kDa on Western blots of wild-type protein extracts; this band was absent in extracts from *dpl-1(n3643)* mutants (Figure 2A).

We used the purified antibodies for immunostaining of fixed worms. The purified antibodies did not stain fixed *dpl-1(n3643)* mutant worms of any stage (data not shown). In wild-type animals, DPL-1 protein was expressed in most and perhaps all cells throughout development and was localized to nuclei. The P(3–8).p nuclei and nuclei of the hypodermal syncytium, hyp7, two proposed sites of synMuv gene function during vulval development (Herman and Hedgecock, 1990; Hedgecock and Herman, 1995; Thomas and Horvitz, 1999), both expressed DPL-1 (Figure 2B and data not shown). DPL-1 was also present in the descendants of P(3–8).p (Figure 2C). In addition to somatic nuclei, immature germ cell and oocyte nuclei were also sites of strong DPL-1 expression (Figure 2D).

We assessed the maternal contribution of DPL-1 protein by staining *dpl-1(n3643)* homozygous progeny of heterozygous *dpl-1(n3643)/+* mothers. DPL-1 was present in *dpl-1(n3643)* embryos but was absent from *dpl-1 (n3643)* larvae generated by *dpl-1(n3643)/+* mothers (Figure 2E and data not shown). These results suggest that maternally provided DPL-1 protein or DPL-1 protein synthesized from maternally provided RNA is present during embryonic development but does not persist at comparable levels into larval development.

Some Neuroblast Divisions Are Affected by Loss of *dpl-1* Function

DP/E2F heterodimers can promote cell cycle progression by activating the transcription of genes required for S phase (reviewed by Lavia and Jansen-Durr, 1999). We, therefore, wanted to determine if loss of *dpl-1* function could prevent cell division. We sought to characterize animals in which both maternally and zygotically provided *dpl-1* activities were severely reduced or eliminated. For this reason, we combined *dpl-1(RNAi)* with the *dpl-1(n3316)* mutation. *dpl-1(RNAi)* effectively reduced the maternal contribution of *dpl-1* activity and DPL-1 protein. First, *dpl-1(RNAi)* eliminated maternal rescue (J. Thomas and H. R. H., unpublished results) of the *dpl-1* synMuv phenotype; 55.1% (n = 156) of *dpl-1 (n2994); lin-15(n433)* mutants descended from *dpl-1 (n2994)/+; lin-15(n433)* mothers were Muv, whereas 100% (n = 147) of *dpl-1(n2994); lin-15(n433)* mutants descended from *dpl-1(n2994)/+; lin-15(n433)* mothers injected with *dpl-1* RNA were Muv. Second, we did not detect DPL-1 protein in embryos descended from mothers injected with *dpl-1* RNA (data not shown).

dpl-1(n3316 RNAi) animals developed into morphologically normal adults. Direct examination and DAPI staining indicated that the cellular divisions that generated many tissues, including the vulva and the gonad, likely occurred normally. To confirm that S phase occurred in generating these postembronically derived structures, we monitored incorporation of the thymidine analog 5-bromo-2′-deoxyuridine (BrdU) (see Experimental Procedures). BrdU was incorporated in the P(3–8).p descendants of *dpl-1(n3316 RNAi)* animals (Figure 3A). We also observed BrdU incorporation in other cells that are generated or that synthesize DNA during the L3 larval stage, including seam cell descendants, germ cell precursors, and intestinal nuclei (Figure 3A and data not shown). These results indicate that loss of *dpl-1* function does not result in a general block in cell division or S phase.

Interestingly, *dpl-1(n3316 RNAi)* animals were uncoordinated (Unc), especially in backward movement. Such Unc mutants are often defective in the generation or function of ventral cord neurons, many of which are postembryonically derived from Pn.a neuroblasts. To

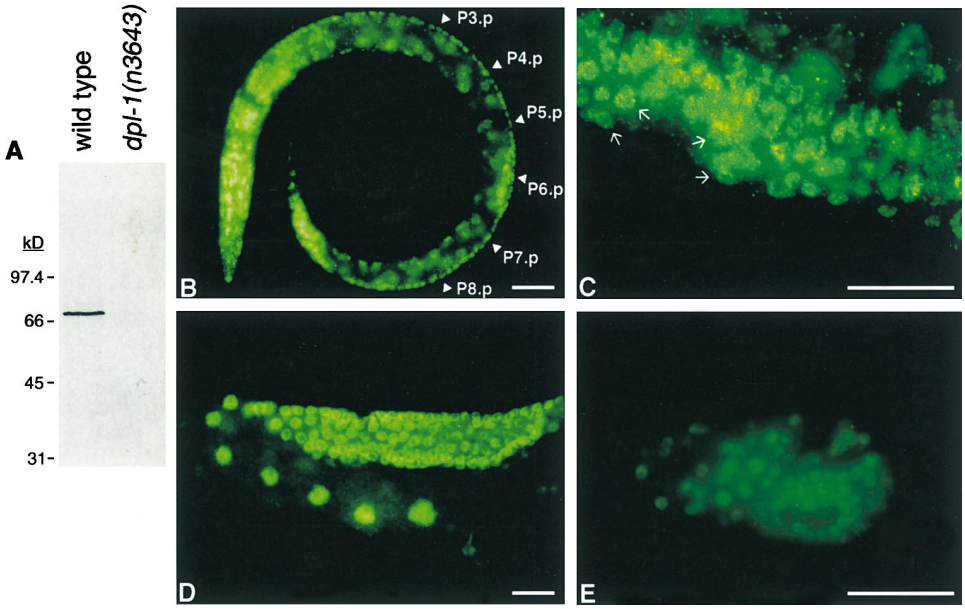

Figure 2. DPL-1 Is Expressed Broadly in Nuclei

(A) Western blot of wild-type and *dpl-1(n3643)* protein extracts with purified anti-DPL-1 antiserum.

(B–E) Whole-mount staining with anti-DPL-1 antiserum. In (B), staining of a wild-type L2 larva is shown. P(3–8).p nuclei are indicated by arrowheads. In (C), DPL-1 expression in nuclei of P(3–8).p descendants (arrows) in a wild-type L4 larva is shown. (D) shows DPL-1 expression in immature germ nuclei and oocyte nuclei of a wild-type adult. (E) shows staining of a *dpl-1(n3643)* pretzel-stage embryo derived from a *dpl-1(n3643)/+* mother. We recognized *dpl-1(n3643)* homozygotes as non-GFP progeny of *dpl-1(n3643)/mIn1*[*dpy-10(e128) mIs14*] mothers. *mIs14*, an integrated transgene linked to the chromosomal inversion *mIn1*, consists of a combination of GFP-expressing transgenes that allow *mIs14*-containing animals to be scored beginning at the 4-cell stage of embryogenesis (M. L. Edgley, J. K. Liu, D. L. Riddle, and A. Fire, personal communication). The scale bar in each panel represents 5 μm.

determine if the number of ventral cord neurons was affected in *dpl-1(n3316 RNAi)* animals, we counted ventral cord nuclei in DAPI-stained individuals. Newly hatched *dpl-1(n3316 RNAi)* and wild-type L1 animals had similar numbers of embryonically derived ventral cord nuclei (Figure 3D). However, the number of ventral cord nuclei in *dpl-1(n3316 RNAi)* adults was substantially reduced as compared to the wild type. Some of the nuclei in *dpl-1(n3316 RNAi)* adults that we scored as ventral cord neurons based on morphology were larger than wild-type ventral cord nuclei and possibly polyploid (Figures 3B and 3C). The reduced number and larger size of postembryonically derived ventral cord nuclei is consistent with a defect in the Pn.a neuroblast lineages (Sulston and Horvitz, 1981).

We directly examined the P(6–10).a lineages of three *dpl-1(n3316 RNAi)* animals. In the wild type, P(6–8).a each generate five neurons, and P(9–10).a each generate four neurons and one cell that undergoes programmed cell death. All 15 of the Pn.a lineages we observed in *dpl-1(n3316 RNAi)* animals were abnormal. In ten cases, the Pn.a cell generated only two cells (Pn.aa and Pn.ap) and in five cases generated only three cells (Pn.aaa, Pn.aap, and Pn.ap). In addition, the times between cell divisions in these mutant lineages were often delayed. For example, the average time between the generation and division of Pn.a cells was 4.5 hr as compared to approximately 2 hr in the wild type (Sulston and Horvitz, 1977). The cells produced by these abnormal lineages often assumed the appearance, as visualized with Nomarski optics, characteristic of terminally differentiated neurons, although some cells retained, often for more than an hour, the clear and swelled appearance of a cell undergoing mitosis. Characteristics of terminally differentiated neurons have previously been observed in undivided cells in mutants with Pn.a cell-lineage defects (Albertson et al., 1978; White et al., 1982). The failure to complete Pn.a lineages in *dpl-1(n3316 RNAi)* animals may reflect a requirement for *dpl-1* activity in cell cycle progression in these lineages.

Identification of Two *C. elegans* E2F-like Genes, *efl-1* and *efl-2*

Since E2F proteins interact with DP family members in mammals, we sought to identify *C. elegans* E2F-like genes. From *C. elegans* EST and genomic sequence databases, we identified two genes, *efl-1* and *efl-2*, that are predicted to encode E2F family proteins. We obtained full-length cDNA clones of *efl-1* and *efl-2* (see supplemental experimental procedures at www.molecule.org/cgi/content/full/7/3/461/DC1) as indicated by the presence of *trans*-spliced leader sequences and poly(A) tails. We deduced the gene structures of *efl-1* and *efl-2* by comparison of genomic DNA and cDNA sequences (Figure 4A).

The EFL-1 protein is similar to mammalian E2F proteins in domains required for DNA binding and for heterodimerization with DP family members (Figure 4B). The DNA binding domains of different mammalian E2F proteins are highly conserved, but the dimerization domains of these proteins are more divergent. The putative dimerization domain of EFL-1 is most similar to the dimer-

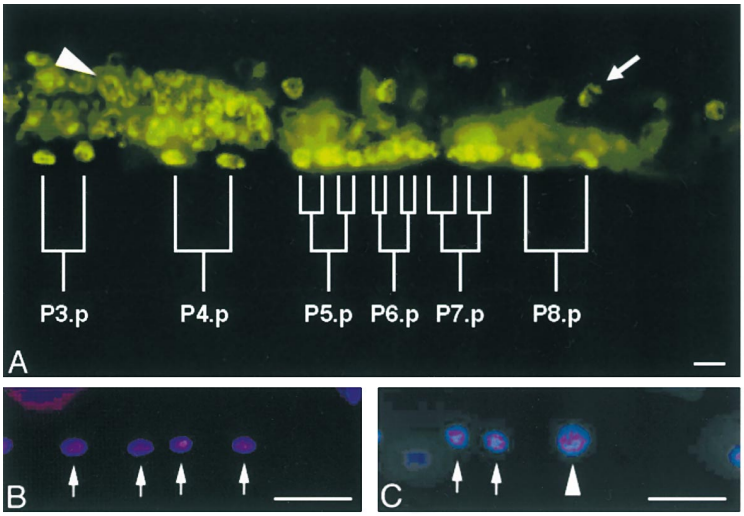

Figure 3. Characterization of P Cell Descendants in *dpl-1(n3316 RNAi)* Animals

(A) BrdU incorporation in L3 stage *dpl-1(n3316 RNAi)* animals. Pn.px and Pn.pxx cells are shown as descendants of their respective Pn.p precursor cells. An intestinal cell nucleus (arrow) and a germ cell nucleus (arrowhead) are indicated. All of these cell types incorporate BrdU in wild-type animals (data not shown). Anterior is to the left and ventral is down.

(B and C) DAPI-stained ventral cord nuclei in wild-type ([B]) and in *dpl-1(n3316 RNAi)* ([C]) animals. Neurons with normal morphology are indicated by arrows; an abnormally large and polyploid neuronal-like nucleus is indicated by an arrowhead.

(D) Numbers of ventral cord nuclei in the wild type and in *dpl-1(n3316 RNAi)* animals. Animals were stained with DAPI, and nuclei between the retrovesicular ganglion and P10.p were counted.

The scale bar in each panel represents 5 μm.

D. *dpl-1(n3316 RNAi)* adults have a reduced number of ventral cord neurons

Genotype	Stage	No. neurons ± SD
wild type	L1	15.0 ± 0.2 (n=36)
dpl-1(n3316 RNAi)	L1	14.9 ± 0.3 (n=30)
wild type	adult	56.3 ± 2.2 (n=48)
dpl-1(n3316 RNAi)	adult	25.5 ± 3.3 (n=44)

ization domains of human E2F-4 (38% identity) and E2F-5 (38%) and less similar to the dimerization domains of E2F-1 (22%), E2F-2 (23%), E2F-3 (26%), and E2F-6 (26%). EFL-1 is also similar to E2F-4 and E2F-5 in that it lacks a nuclear localization signal found in E2F-1, E2F-2, and E2F-3 (Muller et al., 1997; Verona et al., 1997). Because E2F-4 lacks this nuclear localization signal, this protein is proposed to function only when it is recruited to the nucleus, which occurs only in G0 and G1 cells. With the exception of E2F-6, mammalian E2F proteins also have a small carboxy-terminal domain that interacts with pRB, p107, and p130. The EFL-1 carboxyl terminus is similar to those of E2F-1, E2F-2, E2F-3, E2F-4, and E2F-5 but is not similar to that of E2F-6. Together, these comparisons suggest that EFL-1 may interact with LIN-35 Rb and may be most closely related to mammalian E2F-4 and E2F-5.

The putative dimerization domain of EFL-2 is most similar to the dimerization domains of human E2F-3 (31% identity) and E2F-6 (31%) and is somewhat less similar to the dimerization domains of E2F-1 (22%), E2F-2 (24%), E2F-4 (27%), and E2F-5 (25%). The carboxy-terminal region of EFL-2 is similar to the pRB family interaction domains of mammalian E2F proteins. These comparisons indicate that EFL-2 is an E2F family member that may interact with LIN-35 Rb.

efl-1 Is a Class B synMuv Gene

We used RNAi to investigate the functions of *efl-1* and *efl-2*. RNAi of *efl-1* caused a Muv phenotype in *lin-15A (n767)* mutants but not in the wild type or in *lin-15B (n744)* mutants (data not shown), indicating that *efl-1* may be a class B synMuv gene. *efl-1(RNAi)* also caused defects in backward movement similar to those observed in *dpl-1(RNAi)* animals. *efl-2(RNAi)* did not cause Muv or Unc phenotypes in a wild-type background or in either a *lin-15A(n767)* or a *lin-15B(n744)* mutant background (data not shown).

To analyze *efl-1*, we sought deletions that affected the *efl-1* locus (see supplemental experimental procedures at www.molecule.org/cgi/content/full/7/3/461/DC1). We obtained a single allele, *n3318*, that removes 1152 base pairs, deleting 268 base pairs of sequence prior to the putative translation start site and the first three exons (Figure 4A). P(3–8).p cell divisions, germ cell divisions, and adult morphology were all normal in *efl-1(n3318)* mutants (data not shown). We isolated another *efl-1* allele, *n3639* (C. J. C and H. R. H., unpublished results), and found a nonsense mutation predicted to truncate the EFL-1 protein after 174 amino acids (Figures 4B and 4C).

efl-1(n3318) caused a Muv phenotype as a double mutant with *lin-38(n751)*, *lin-15A(n433)*, and *lin-15A(n767)*, all alleles of class A synMuv genes, whereas *efl-1(n3318); lin-15B(n744)* double mutants had wild-type vulvae (Table 1). Expression of the *efl-1* cDNA under its endogenous promoter rescued the Muv phenotype of *efl-1(n3318); lin-15A(n433)* mutants, indicating that the Muv phenotype of these mutants was caused by the *efl-1(n3318)* deletion (see Experimental Procedures). That both the *efl-1(n3318)* mutation and *efl-1(RNAi)* cause a Muv phenotype specifically in the presence of a class A synMuv mutation indicates that *efl-1* is a class B synMuv gene. The class B synMuv activity of *efl-1* is neither redundant with nor is inhibited by *efl-2*, as *efl-2(RNAi)* had little effect on the penetrance of the Muv phenotype of *efl-*

1(n3318); lin-15A(n433) mutants. In addition to the Muv phenotype, *efl-1* mutations caused sterility and embryonic lethality (C. J. C. and H. R. H., unpublished results).

DPL-1 and EFL-1 Interact with Each Other and with LIN-35 In Vitro

Since mammalian DP, E2F, and pRB family proteins physically interact, we sought to determine if DPL-1, EFL-1, and LIN-35 likewise associate. We were specifically interested in understanding the consequences of the *dpl-1(n3643)* mutation on DPL-1 protein–protein interactions. *n3643* introduces a stop codon that is predicted to truncate DPL-1 after 340 amino acids. Western blots of extracts from *dpl-1(n3643)* mutants with crude DPL-1 antiserum indicate that this truncated protein is stably expressed in vivo (C. J. C. and H. R. H., unpublished results). The truncated protein retains domains similar to those used by DP family members for both DNA and E2F binding. Although these domains are present in the truncated protein, *dpl-1(n3643); lin-15A(n433)* mutants are partially defective in vulval development (Table 1).

To assess DPL-1 protein–protein interactions in *dpl-1(n3643)* mutants, we compared binding properties of a DPL-1 amino-terminal fragment to those of a DPL-1 carboxy-terminal fragment. We found that GST-tagged DPL-1(31–343) but not GST-DPL-1(344–598) bound in vitro–translated EFL-1 (Figure 5A). Therefore, DPL-1 and EFL-1 can interact, and this interaction may be mediated by a domain of DPL-1 that is similar to the domain of mammalian DP-1 important for interaction with E2F proteins.

We next tested for interactions of DPL-1 fragments with LIN-35 Rb. The 961-amino acid LIN-35 protein contains a domain (amino acids 496–897) that is similar to the A/B pocket, a protein–protein interaction domain of pRB, p107, and p130 (Lu and Horvitz, 1998). GST-DPL-1(31–343) did not bind either LIN-35(1–555) or LIN-35(270–961) fragments (Figure 5A). However, GST-DPL-1(344–598) specifically bound the LIN-35(270–961) fragment (Figure 5A), indicating that the interaction of GST-DPL-1(344–598) with LIN-35 is dependent on a carboxy-terminal region of LIN-35. Together these results indicate that a DPL-1 amino-terminal domain interacts with EFL-1, and a DPL-1 carboxy-terminal domain interacts with the LIN-35 Rb carboxyl terminus.

We next tested the interaction between EFL-1 and LIN-35 Rb. GST-EFL-1(214–342) interacted in vitro with LIN-35(270–961) (Figure 5B). Like the interaction of LIN-35 Rb with GST-DPL-1(344–598), this interaction was dependent upon a carboxy-terminal region of LIN-35 Rb, since LIN-35(1–555) did not bind GST-EFL-1(214–342) (Figure 5B). We propose that the carboxy-terminal tail of EFL-1 binds the predicted A/B pocket domain of LIN-35 Rb.

We also examined the possible formation of a DPL-1/EFL-1/LIN-35 ternary complex. To address this issue, we asked whether GST-DPL-1(31–343), which does not interact directly with LIN-35(270–961), would in the presence of EFL-1 associate with LIN-35(270–961). When incubated in a single binding reaction, both EFL-1 and LIN-35(270–961) associated with GST-DPL-1(31–343) (Figure 5C). These interactions indicate the formation of a GST-DPL-1(31–343)/EFL-1/LIN-35(270–961) ternary complex.

Together these results suggest that DPL-1 and EFL-1 interact with each other and with LIN-35 Rb in vivo. We speculate that the mutant DPL-1/EFL-1 heterodimer in *dpl-1(n3643)* animals interacts with LIN-35 Rb only through EFL-1 and that the affinity of this interaction is not sufficient for the full function of a DPL-1/EFL-1/LIN-35 complex during vulval development. It is possible that the truncated DPL-1 protein in *dpl-1(n3643)* mutants is defective in another putative DPL-1 function, for example DNA binding, and that this defect contributes to an impaired DPL-1/EFL-1/LIN-35 complex function.

RTK/Ras Pathway Activity Is Required for *dpl-1* and *efl-1* Muv Phenotypes

We conducted genetic epistasis tests to investigate the relationship between *dpl-1* and *efl-1* and genes involved in RTK/Ras signaling. Animals bearing *dpl-1(n3316)* and *lin-15A(n767)* mutations as well as either *sem-5* Grb2, *let-60* Ras, *lin-45* Raf, or *mpk-1* MAPK mutant alleles were Vul, indicating that RTK/Ras pathway activity is required for the *dpl-1(n3316); lin-15A(n767)* Muv phenotype. (A *dpl-1* double mutant with *let-23* RTK was not constructed because of tight linkage and a lack of suitable markers.) We also observed a Vul phenotype in triple mutants containing *efl-1(n3318)* and *lin-15A(n767)* as well as either *let-23* RTK, *sem-5* Grb2, *let-60* Ras, *lin-45* Raf, or *mpk-1* MAPK alleles. These data suggest that *dpl-1* and *efl-1* act upstream of or in parallel to the RTK/Ras pathway in vulval development.

By contrast, *dpl-1(n3316); lin-3* EGF*; lin-15A(n767)* and *lin-3* EGF*; efl-1(n3318); lin-15A(n767)* triple mutants were Muv. *lin-3* encodes an EGF-like protein that presumably binds LET-23 RTK and activates RTK/Ras signaling in P(5–7).p (Hill and Sternberg, 1992). In *lin-3* mutants, RTK/Ras signaling is not activated, and P(5–7).p do not adopt vulval cell fates (Horvitz and Sulston, 1980). Consistent with our observations, previous studies have shown that other synMuv mutants do not require either *lin-3* function or the gonadal anchor cell, the source of LIN-3 protein, for expression of a Muv phenotype (Ferguson et al., 1987; Sternberg and Horvitz, 1989; Lu and Horvitz, 1998).

There are at least two possible explanations why P(3–8).p can adopt vulval cell fates when *dpl-1*, *efl-1*, and other synMuv mutations are combined with a *lin-3* mutation but cannot adopt vulval cell fates when *dpl-1*, *efl-1*, and other synMuv mutations are combined with RTK/Ras pathway mutations. Both explanations assume that some RTK/Ras signaling can occur in a ligand-independent fashion, that is, in a *lin-3* mutant. First, loss of synMuv function may result in ectopic activation of RTK/Ras signaling via a *lin-3*-independent mechanism to a level that is sufficient to induce vulval cell fates. Alternatively, loss of synMuv function may lower the threshold of activity required for vulval cell fate specification to a point that can be exceeded by basal, uninduced RTK/Ras pathway activity. In either case, these results indicate that *dpl-1* and *efl-1* can affect cell-fate determination not only in P3.p, P4.p, and P8.p but also in P(5–7).p.

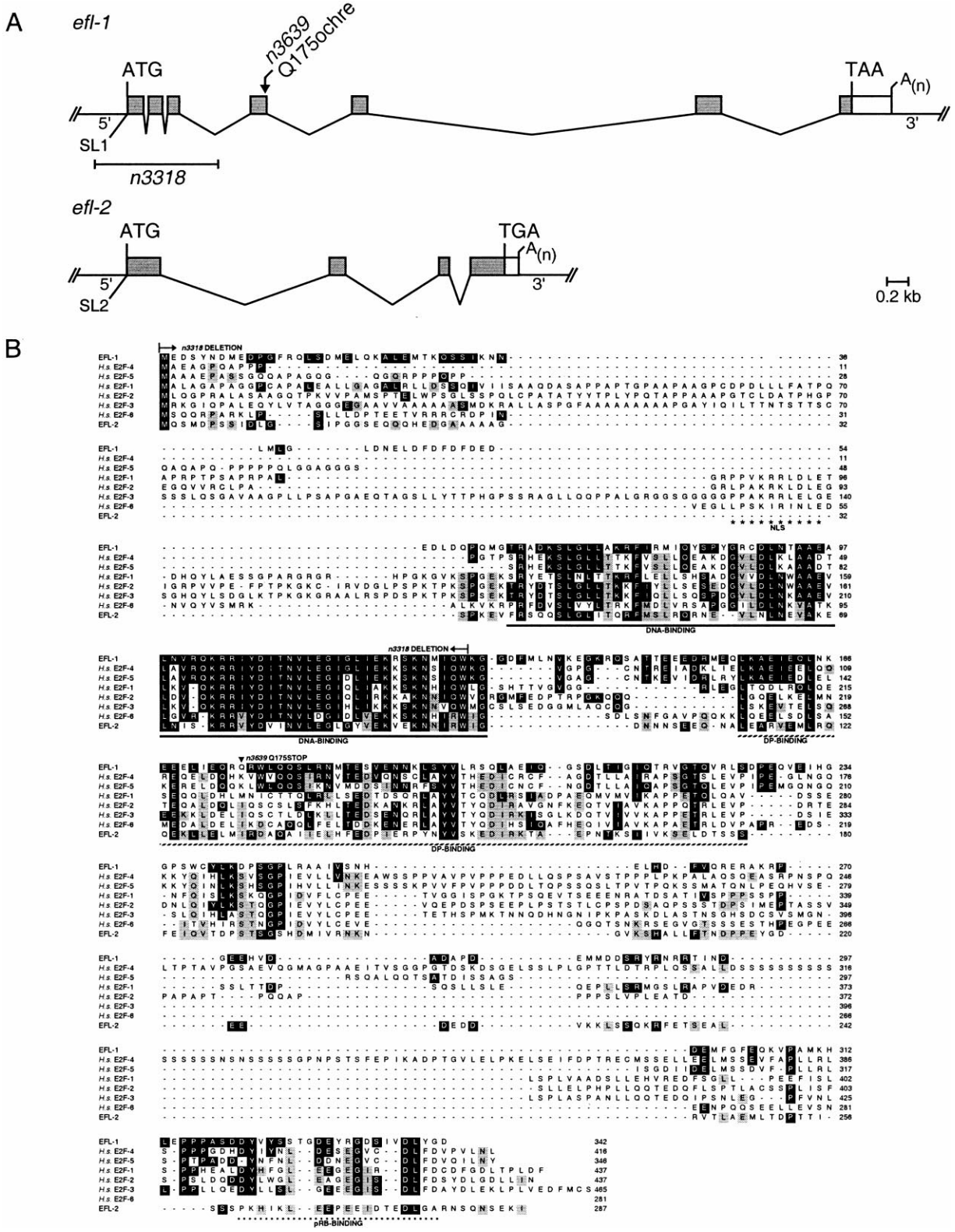

Figure 4. Identification of *efl-1* and *efl-2*

(A) Gene structures of *efl-1* and *efl-2* as deduced from cDNA and genomic sequences. Coding sequences are shaded. Translation initiation and termination codons, SL1 and SL2 *trans*-spliced leaders, and poly(A) tails are indicated. The region deleted in *efl-1(n3318)* mutants is bracketed.

(B) Alignment of EFL-1 and EFL-2 with human E2F proteins (human E2F-4, GenBank accession number NP_001941; E2F-5, NP_001942; E2F-1, Q01094; E2F-2, NP_004082; E2F-3, NP_001940; and E2F-6, O75461). Solid boxes indicate identities between EFL-1 and another protein.

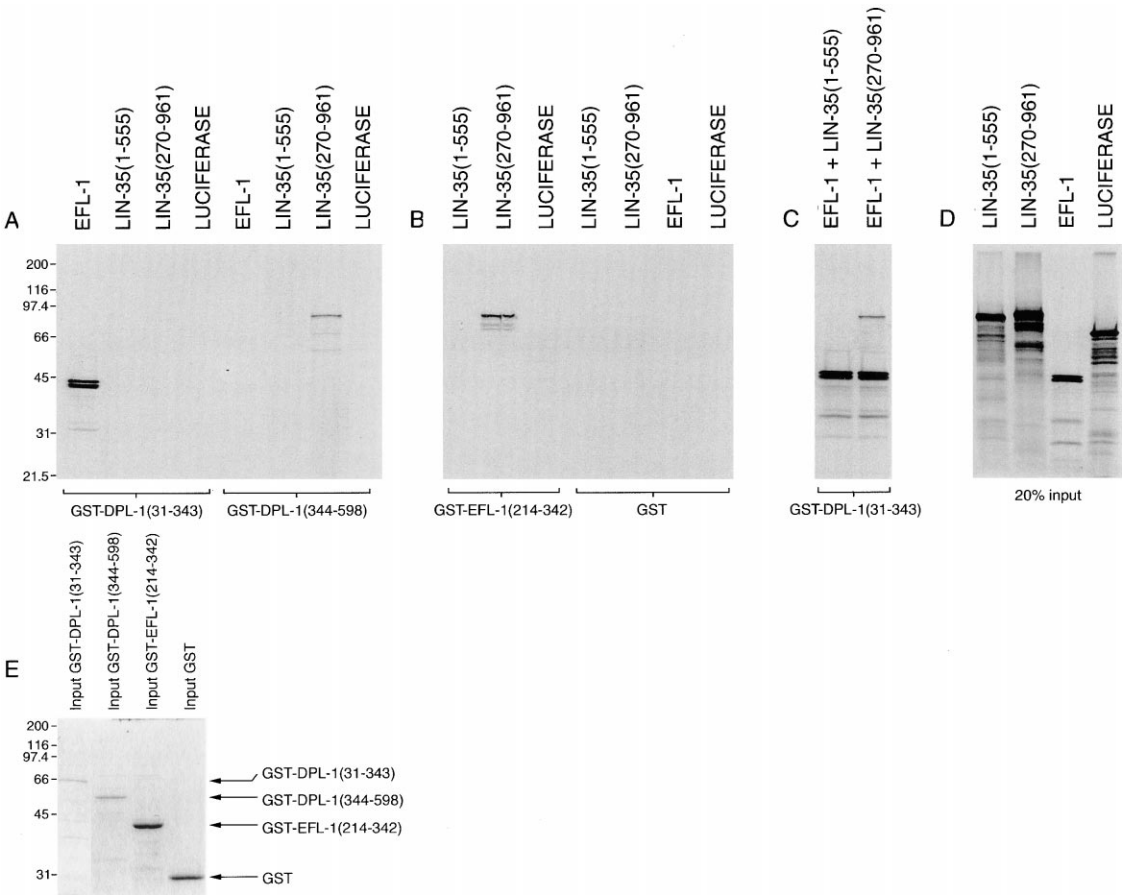

Figure 5. DPL-1, EFL-1, and LIN-35 In Vitro Interactions

(A) The DPL-1 amino terminus interacted with EFL-1, and the DPL-1 carboxyl terminus interacted with LIN-35. GST-DPL-1 (amino acids 31–343) and GST-DPL-1 (amino acids 344–598) were incubated with ^{35}S-labeled EFL-1, LIN-35 (amino acids 1–555), LIN-35 (amino acids 270–961), and luciferase.

(B) The EFL-1 carboxyl terminus interacted with LIN-35. GST-EFL-1 (amino acids 214–342) was incubated with ^{35}S-labeled LIN-35(1–555), LIN-35(270–961), and luciferase. None of the ^{35}S-labeled proteins interacted with GST alone.

(C) LIN-35 interaction with the DPL-1 amino terminus was dependent on EFL-1. GST-DPL-1(31–343) was incubated with ^{35}S-labeled EFL-1 and LIN-35(1–555) and with ^{35}S-labeled EFL-1 and LIN-35(270–961).

(D) Twenty percent of the ^{35}S-labeled proteins used in the binding reactions is shown.

(E) Coomassie blue staining of purified GST-DPL-1(31–343), GST-DPL-1(344–598), GST-EFL-1(214–342), and GST proteins used in the binding reactions.

Binding reactions ([A]–[C]) were performed as described by Reddien and Horvitz (2000). ^{35}S-labeled bound proteins ([A]–[C]) or input proteins ([D]) were resolved by 10% SDS–PAGE and analyzed by autoradiography. GST-tagged proteins ([E]) were resolved by 10% SDS–PAGE and stained with Coomassie blue.

Discussion

DPL-1 and EFL-1 May Repress Rather Than Promote Transcription during Vulval Development

A number of proteins with class B synMuv activity are similar to proteins implicated in chromatin modification, nucleosome remodeling, and transcriptional repression. In mammals, pRB regulates expression of DP/E2F-responsive genes, in part, by recruiting the histone deacetylase HDAC1 (Brehm et al., 1998; Luo et al., 1998; Magnaghi-Jaulin et al., 1998). A pRB-associated complex that includes HDAC1 and an associated subunit, RbAp48, has been shown to deacetylate polynucleosomal substrates in vitro, reflecting a role of this complex in pRB-mediated repression (Nicolas et al., 2000). The *C. elegans* counterparts of these proteins, LIN-35 Rb, HDA-1 HDAC, and LIN-53 p48, physically interact in vitro and act together in vulval development, indicating that a functional relationship as transcriptional repressors may be conserved (Lu and Horvitz, 1998). Other studies have suggested that RBA-1, CHD-3, CHD-4, and EGR-1, proteins similar to components of the NURD

Shaded boxes indicate identities between EFL-2 and a human E2F protein. EFL-1 sequence removed by *n3318* is indicated by brackets. The DNA binding (solid lines), DP binding (hatched lines), and pRB binding (dotted line) domains and the nuclear localization signals (NLS; asterisks) of mammalian E2F proteins are indicated.

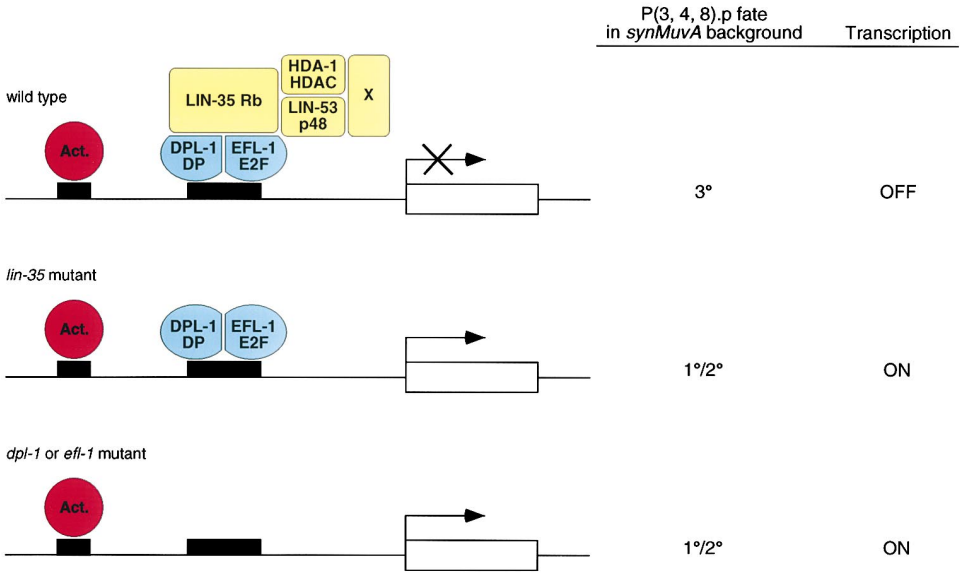

Figure 6. Model: DPL-1 and EFL-1 May Repress but Not Activate Transcription

DNA sequences bound by transcription factors are indicated by black boxes, and a representative vulval specification gene is shown as an open box. In this model, a DPL-1/EFL-1 heterodimer tethers LIN-35 Rb and a complex containing LIN-53 p48, HDA-1 HDAC, and proteins that repress transcription, denoted as "X", to DNA. In wild-type P3.p, P4.p, and P8.p cells (top), this complex is active and represses transcription of vulval specification genes. In *lin-35; synmuvA* mutants (middle), the transcriptional repressor complex is uncoupled from DPL-1/EFL-1, and transcription of vulval specification genes is activated. Since P3.p, P4.p, and P8.p adopt 1°/2° fates in *dpl-1; synmuvA* and *efl-1; synmuvA*, we propose that vulval specification genes are also activated in these mutants, presumably by another transcriptional activator denoted here as "Act." (bottom).

(nucleosome remodeling and histone deacetylase) complex, may also act in synMuv-mediated repression (Solari and Ahringer, 2000; Walhout et al., 2000).

By analogy to their mammalian counterparts, DPL-1 and EFL-1 may form a heterodimer and bind DNA to modulate gene expression by tethering to DNA a protein complex containing LIN-35 Rb, LIN-53 p48, HDA-1 HDAC, and other proteins (Figure 6). Since the mammalian counterparts of LIN-35, LIN-53, and HDA-1 appear to function as transcriptional repressors, we propose that DPL-1 and EFL-1 target a repressor complex to genes required in P(3–8).p for vulval cell-fate specification, thereby antagonizing Ras signaling during vulval development. In this model, the transcription of genes required for vulval specification is ectopically activated in synMuv mutants; that is, such genes are transcribed in *dpl-1* and *efl-1* loss-of-function mutants (Figure 6). Consequently, while DPL-1/EFL-1 activity may be important for repression of target genes, we propose that, at least in the context of vulval development, DPL-1/EFL-1 activity does not appear to be required for activation of these same targets.

dpl-1 and *efl-1* Antagonize RTK/Ras Signaling

Mammalian Rb and Ras can act antagonistically to regulate the G1-to-S phase transition (Mittnacht et al., 1997; Peeper et al., 1997), and E2F-4 and E2F-5 can function redundantly in mouse embryonic fibroblasts to oppose the effects of Ras on S phase entry (Gaubatz et al., 2000). In *C. elegans*, *dpl-1* and *efl-1* normally inhibit, whereas RTK/Ras signaling normally promotes, vulval cell-fate specification. Therefore, *dpl-1* and *efl-1* antagonize RTK/Ras pathway function in vulval development. As discussed above, the function of DPL-1 and EFL-1 as transcriptional repressors may be important for the regulation of vulval development, and, consequently, for the antagonism of Ras signaling. It is possible that DPL-1/EFL-1 heterodimers converge on the same targets as controlled by the *let-23* RTK/*let-60* Ras–regulated LIN-1 ETS and LIN-31 winged helix transcription factors. LIN-1 and LIN-31 form a protein complex that inhibits vulval induction; when phosphorylated by MPK-1 MAPK, this complex dissociates to release phosphorylated LIN-31, which is believed to promote vulval cell-fate specification (Tan et al., 1998). That RTK/Ras pathway activity is required for vulval cell-fate specification in *dpl-1* and *efl-1* mutants is consistent with the requirement for LIN-31 phosphorylation and activation by RTK/Ras: loss of *dpl-1* or *efl-1* function in the absence of RTK/Ras signaling would not activate transcription by an unphosphorylated LIN-31 protein. However, the existing data do not preclude models in which *dpl-1* and *efl-1* antagonize RTK/Ras signaling at another point in the pathway.

Comparisons of EFL-1 with Mammalian E2F Family Members

Although E2F-1, E2F-2, E2F-3, E2F-4, and E2F-5 all have transactivation and pRB family protein binding domains and, hence, might all function in both transcriptional activation and repression, it is possible that each E2F protein performs only one of these functions in vivo. E2F-4 and E2F-5 may act primarily in repression. Specifically, E2F-4 is present at the promoters of DP/E2F-

responsive genes in G0 and in early G1, when these genes are repressed (Takahashi et al., 2000). In addition, *E2f4* and *E2f5* single- and *E2f4 E2f5* double-mutant mice exhibit defects in cellular differentiation events that are thought to be caused by the loss of E2F4 and E2F5 repressor complexes with pRb, p107, and p130 (Lindeman et al., 1998; Gaubatz et al., 2000; Humbert et al., 2000; Rempel et al., 2000). EFL-1 is structurally most similar to the mammalian E2F-4 and E2F-5 proteins. The role we propose for EFL-1 as a transcriptional repressor during vulval development is similar to the suspected roles of E2F-4 and E2F-5.

Are *dpl-1* DP and *efl-1* E2F Required for Entry into S Phase?

Considerable evidence indicates that mammalian DP and E2F proteins can promote the entry of cells into S phase, thereby stimulating cell cycle progression. Our observations of *dpl-1(n3316 RNAi)* animals, which are presumably deficient in both the zygotic and maternal contribution of DPL-1, suggest that DPL-1 activity is not essential in every cell for cell cycle progression. Since *dpl-1* is the only predicted *C. elegans* DP family member, and since DP protein function is thought to be necessary for DP/E2F heterodimer function, DP/E2F activity in *C. elegans* may not be generally required for cell cycle progression. However, *dpl-1* and *efl-1* may be required to promote S phase entry in some cell types. Specifically, the Pn.a neuroblasts of *dpl-1(n3316 RNAi)* animals did not complete their divisions and sometimes generated large polyploid descendants. We conclude that *dpl-1* and possibly *efl-1* may act in but are not essential for the cell cycle in *C. elegans*. We note the possibility that undetectable levels of *dpl-1* activity and DPL-1 protein may be present in *dpl-1(n3316 RNAi)* animals and may fulfill a broader requirement for *dpl-1* in promoting cell cycle progression.

As discussed above, loss-of-function mutations in *dpl-1* and *efl-1*, like loss-of-function mutations in *lin-35* Rb, cause cell-fate transformations that result in supernumerary cell divisions in the P(3,4,8).p lineages. The extra cell divisions in these mutants are consistent with the possibility that a DPL-1/EFL-1/LIN-35 protein complex normally inhibits cell cycle progression in P(3,4,8).p. Thus, while *dpl-1* and *efl-1* promote cell division in some cell types, e.g., in Pn.a descendants, *dpl-1* and *efl-1* may prevent cell division in other cell types, e.g., in P(3,4,8).p descendants.

While it is tempting to speculate that *dpl-1* and *efl-1* are cell cycle regulators in *C. elegans*, we do not yet know if the effects of these genes on cell division are caused by the direct regulation of the cell cycle machinery or are caused by the regulation of cell fate–determining factors that subsequently impinge on the cell cycle machinery. We hope that further studies of *dpl-1* and *efl-1* mutants will help establish the in vivo functions not only of these *C. elegans* genes but also of DP and E2F genes in other organisms, including humans.

Experimental Procedures

Strains

All strains were cultured at 20°C on NGM agar seeded with *E. coli* strain OP50 as described by Brenner (1974). Bristol N2 was the wild-type strain. Mutant alleles used are listed below and are described by Riddle et al. (1997) unless noted otherwise: LGII *dpy-10(e128)*, *dpl-1(n2994, n3316, n3643)* (J. Thomas and H. R. H., unpublished results; this study); *let-23(sy97)*, *unc-4(e120)*, *lin-38(n751)*, *mnC1*[*dpy-10(e128) unc-52(e444)*] (Herman, 1978); *mIn1*[*dpy-10(e128) mIs14*] (M. L. Edgley, J. K. Liu, D. L. Riddle, and A. Fire, personal communication); LGIII *mpk-1(oz140)*, *dpy-17(e164)*; LGIV *lin-45(sy96)*; *lin-3(n378)*; *let-60(n2021)*; LGV *rol-4(sc8)*, *unc-76(e911)*, *efl-1(n3318, n3639)* (this study); *dpy-21(e428)*; LGX *sem-5(n2030)*, *lin-15B(n744)*, *lin-15A(n433)* (Ferguson and Horvitz, 1989); and *lin-15A(n767)*. The deficiency *mnDf67* was also used (Sigurdson et al., 1984). *dpl-1(n3643)* and *efl-1(n3639)* were isolated in a screen for mutations that caused a Muv phenotype in a *lin-15A(n767)* background (C. J. C., F. Stegmeier, and H. R. H., unpublished results).

Antibody Preparation and Immunocytochemistry

Crude anti-DPL-1 antiserum was provided by B. Page and J. Priess. This antiserum was generated by injecting purified 6His-DPL-1(294–598) into rabbits. We affinity-purified anti-DPL-1 antibodies by applying this antiserum to nitrocellulose strips containing GST-DPL-1(344–598) fusion protein, and we washed and eluted bound antibody as described by Koelle and Horvitz (1996). Antibodies were further purified by preadsorption to an acetone precipitate of proteins from *dpl-1(n3643)* mutant animals that was prepared essentially as described by Harlow and Lane (1988). Antibodies were used at a 1:500 dilution on Western blots. Larvae and adults for whole-mount staining were fixed for 30 min as described by Nonet (1997), and embryos were fixed for 30 min as described by Finney and Ruvkun (1990). Fixed animals were incubated with affinity-purified preadsorbed DPL-1 antibodies at a 1:50 dilution, and FITC-conjugated goat anti-rabbit secondary antibody (Jackson Laboratories) was used for detection.

RNAi Analyses

Templates for in vitro transcription reactions were made by PCR amplification of full-length *dpl-1*, *efl-1*, and *efl-2* cDNA inserts and their flanking T3 and T7 promoter sequences. In vitro–transcribed RNA was annealed and injected as described by Fire et al. (1998). Injected animals were transferred 10–15 hr after injection, and their progeny were analyzed. The *dpl-1* gene is located within a large intron of the gene T23G7.2. To determine if *dpl-1* mutations or *dpl-1(RNAi)* perturb T23G7.2 function, we performed RNA interference of T23G7.2. T23G7.2*(RNAi)* animals did not display the Muv, Unc, or sterile phenotypes caused by *dpl-1(RNAi)* or by *dpl-1* mutations.

BrdU Incorporation and Detection

BrdU application and detection were performed as described by Boxem et al. (1999), except that BrdU was applied to *dpl-1(n3316 RNAi) unc-4(e120)* L2 larvae after ventral cord divisions had been completed, and animals were harvested as L3 larvae after P(3–8).p divisions had commenced.

Cell Lineage Analysis

Animals were mounted for Nomarski microscopy and observed as described by Sulston and Horvitz (1977) for at least 4 hr following recovery from lethargus, during which time most nuclei in *dpl-1(n3316 RNAi)* animals adopted morphologies like those of differentiated neurons.

Transgenic Strains

Germline transformations were performed as described by Mello et al. (1991). For rescue of the *dpl-1(n2994); lin-15A(n433)* Muv phenotype, we injected C32F7 (10 ng/μl) or a 5.2 kb PvuII-PvuII subclone of C32F7 (50 ng/μl) with pRF4 (80 ng/μl) as a coinjection marker. Expression of the mutant *rol-6* gene encoded by pRF4 causes a roller (Rol) phenotype (Mello et al., 1991). 3/3 C32F7 and 4/4 5.2 kb PvuII-PvuII subclone transgenic lines were rescued. To rescue the Ste phenotype caused by *dpl-1(n3316)*, we injected *dpl-1(n3316) unc-4(e120)/mnC1* mutants with C32F7 (10 ng/μl) and pRF4 (80 ng/μl). We recovered F1 and F2 transgenic Unc animals, which themselves produced dead eggs and rare live transgenic Unc progeny. To rescue the Muv phenotype of *efl-1(n3318); lin-15A(n433)* mutants, we used pEFL-1.MG, a minigene construct containing the

efl-1 cDNA flanked by 1.8 kb of upstream genomic sequence and 2.1 kb of downstream genomic sequence. pEFL-1.MG (50 ng/μl) and the coinjection marker pPD93.97 (80 ng/μl), which contains *gfp* under the control of the *myo-3* promoter, were injected into + *unc-76(e911) efl-1(n3318)* +/*rol-4(sc8)* + + *dpy-21(e428)*; *lin-15A(n433)* animals. Unc animals of transgenic lines were scored, and 5/6 lines were rescued for the Muv phenotype. To obtain genomic DNA clones of the *efl-1* locus, we used an *efl-1* cDNA fragment to screen a library of *C. elegans* genomic DNA cloned into the λ2001 vector (A. Coulson, personal communication). We obtained two clones, λE4-1 and λE11-1, that together spanned the *efl-1* locus. To rescue the Ste Mel phenotype caused by *efl-1(n3318)*, we injected + *unc-76(e911) efl-1(n3318)* +/*rol-4(sc8)* + + *dpy-21(e428)* mutants with λE4-1 (20 ng/μl), λE11-1 (20 ng/μl), and pPD93.97 (80 ng/μl). 5/7 Unc transgenic lines were rescued.

In Vitro Binding Experiments

Constructs encoding GST-DPL-1(31–343) and GST-DPL-1(344–598) were made by subcloning portions of the *dpl-1* cDNA into pGEX-5X-1 and pGEX-3X (Pharmacia), respectively. The construct encoding GST-EFL-1(214–342) was made by subcloning a portion of the *efl-1* cDNA into pGEX-2T (Pharmacia). Fusion proteins were expressed in BL21(DE3) cells and purified using glutathione Sepharose resin according to the manufacturer's recommendations (Pharmacia). A portion of the *efl-1* cDNA encoding amino acids 8–342 was cloned into pCITE-4a(+) (Novagen). Constructs encoding LIN-35(1–555) and LIN-35(270–961) were described previously (Lu and Horvitz, 1998). These constructs were used as templates for in vitro synthesis of ^{35}S-labeled proteins (TNT Coupled Reticulocyte Lysate System, Promega). Binding experiments were performed as described by Reddien and Horvitz (2000), and bound proteins were analyzed by SDS–PAGE and autoradiography.

Acknowledgments

We thank Mark Alkema, Scott Cameron, Ewa Davison, Brad Hersh, Jackie Lees, and Eric Miska for comments concerning this manuscript; Mark Metzstein and Jeff Thomas for helpful discussions during the course of this work; and Barbara Page and Jim Priess for providing crude anti-DPL-1 antiserum and for communicating results prior to publication. We also thank Frank Stegmeier for assistance in isolating *dpl-1(n3643)* and *efl-1(n3639)*; Beth Castor for DNA sequence determination; Na An for strain management; Rajesh Ranganathan, Peter Reddien, and other members of the Horvitz laboratory for constructing the deletion library; Alan Coulson for the λ genomic library; Andy Fire for pPD93.97; Yuji Kohara for cDNA clones; Peter Okkema for *C. elegans* cDNA libraries; the *C. elegans* Genome Sequencing Consortium for genome sequence of the *dpl-1* and *efl-2* loci; and the *C. elegans* Genetics Center for strains used in this work. This work was supported by NIH grant GM24663. C. J. C. was a Koch Graduate Fellow. H. R. H. is an Investigator of the Howard Hughes Medical Institute.

Received September 29, 2000; revised February 19, 2001.

References

Albertson, D.G., Sulston, J.E., and White, J.G. (1978). Cell cycling and DNA replication in a mutant blocked in cell division in the nematode *Caenorhabditis elegans*. Dev. Biol. *63*, 165–178.

Boxem, M., Srinivasan, D.G., and van den Heuvel, S. (1999). The *Caenorhabditis elegans* gene *ncc-1* encodes a cdc2-related kinase required for M phase in meiotic and mitotic cell divisions, but not for S phase. Development *126*, 2227–2239.

Brehm, A., Miska, E.A., McCance, D.J., Reid, J.L., Bannister, A.J., and Kouzarides, T. (1998). Retinoblastoma protein recruits histone deacetylase to repress transcription. Nature *391*, 597–601.

Brenner, S. (1974). The genetics of *Caenorhabditis elegans*. Genetics *77*, 71–94.

C. elegans Sequencing Consortium. (1998). Genome sequence of the nematode *C. elegans*: a platform for investigating biology. Science *282*, 2012–2018.

Clark, S.G., Lu, X., and Horvitz, H.R. (1994). The *Caenorhabditis elegans* locus *lin-15*, a negative regulator of a tyrosine kinase signaling pathway, encodes two different proteins. Genetics *137*, 987–997.

Dyson, N. (1998). The regulation of E2F by pRB-family proteins. Genes Dev. *12*, 2245–2262.

Ferguson, E.L., and Horvitz, H.R. (1989). The multivulva phenotype of certain *Caenorhabditis elegans* mutants results from defects in two functionally redundant pathways. Genetics *123*, 109–121.

Ferguson, E.L., Sternberg, P.W., and Horvitz, H.R. (1987). A genetic pathway for the specification of the vulval cell lineages of *Caenorhabditis elegans*. Nature *326*, 259–267.

Finney, M., and Ruvkun, G. (1990). The *unc-86* gene product couples cell lineage and cell identity in *C. elegans*. Cell *63*, 895–905.

Fire, A., Xu, S., Montgomery, M.K., Kostas, S.A., Driver, S.E., and Mello, C.C. (1998). Potent and specific genetic interference by double-stranded RNA in *Caenorhabditis elegans*. Nature *391*, 806–811.

Gaubatz, S., Lindeman, G.J., Ishida, S., Jakoi, L., Nevins, J.R., Livingston, D.M., and Rempel, R.E. (2000). E2F4 and E2F5 play an essential role in pocket protein-mediated G1 control. Mol. Cell *6*, 729–735.

Girling, R., Partridge, J.F., Bandara, L.R., Burden, N., Totty, N.F., Hsuan, J.J., and La Thangue, N.B. (1993). A new component of the transcription factor DRTF1/E2F. Nature *362*, 83–87.

Harlow, E., and Lane, D.P. (1988). Antibodies: A Laboratory Manual. (Cold Spring Harbor, NY: Cold Spring Harbor Laboratory Press).

Hedgecock, E.M., and Herman, R.K. (1995). The *ncl-1* gene and genetic mosaics of *Caenorhabditis elegans*. Genetics *141*, 989–1006.

Helin, K., Wu, C.L., Fattaey, A.R., Lees, J.A., Dynlacht, B.D., Ngwu, C., and Harlow, E. (1993). Heterodimerization of the transcription factors E2F-1 and DP-1 leads to cooperative *trans*-activation. Genes Dev. *7*, 1850–1861.

Herman, R.K. (1978). Crossover suppressors and balanced recessive lethals in *Caenorhabditis elegans*. Genetics *88*, 49–65.

Herman, R.K., and Hedgecock, E.M. (1990). Limitation of the size of the vulval primordium of *Caenorhabditis elegans* by *lin-15* expression in surrounding hypodermis. Nature *348*, 169–171.

Hill, R.J., and Sternberg, P.W. (1992). The gene *lin-3* encodes an inductive signal for vulval development in *C. elegans*. Nature *358*, 470–476.

Horvitz, H.R., and Sulston, J.E. (1980). Isolation and genetic characterization of cell-lineage mutants of the nematode *Caenorhabditis elegans*. Genetics *96*, 435–454.

Hsieh, J., Liu, J., Kostas, S.A., Chang, C., Sternberg, P.W., and Fire, A. (1999). The RING finger/B-box factor TAM-1 and a retinoblastoma-like protein LIN-35 modulate context-dependent gene silencing in *Caenorhabditis elegans*. Genes Dev. *13*, 2958–2970.

Huang, L.S., Tzou, P., and Sternberg, P.W. (1994). The *lin-15* locus encodes two negative regulators of *Caenorhabditis elegans* vulval development. Mol. Biol. Cell *5*, 395–411.

Humbert, P.O., Rogers, C., Ganiatsas, S., Landsberg, R.L., Trimarchi, J.M., Dandapani, S., Brugnara, C., Erdman, S., Schrenzel, M., Bronson, R.T., and Lees, J.A. (2000). E2F4 is essential for normal erythrocyte maturation and neonatal viability. Mol. Cell *6*, 281–291.

Koelle, M.R., and Horvitz, H.R. (1996). EGL-10 regulates G protein signaling in the *C. elegans* nervous system and shares a conserved domain with many mammalian proteins. Cell *84*, 115–125.

Lavia, P., and Jansen-Durr, P. (1999). E2F target genes and cell-cycle checkpoint control. Bioessays *21*, 221–230.

Lindeman, G.J., Dagnino, L., Gaubatz, S., Xu, Y., Bronson, R.T., Warren, H.B., and Livingston, D.M. (1998). A specific, nonproliferative role for E2F-5 in choroid plexus function revealed by gene targeting. Genes Dev. *12*, 1092–1098.

Lu, X., and Horvitz, H.R. (1998). *lin-35* and *lin-53*, two genes that antagonize a *C. elegans* Ras pathway, encode proteins similar to Rb and its binding protein RbAp48. Cell *95*, 981–991.

Luo, R.X., Postigo, A.A., and Dean, D.C. (1998). Rb interacts with histone deacetylase to repress transcription. Cell *92*, 463–473.

Magnaghi-Jaulin, L., Groisman, R., Naguibneva, I., Robin, P., Lorain,

S., Le Villain, J.P., Troalen, F., Trouche, D., and Harel-Bellan, A. (1998). Retinoblastoma protein represses transcription by recruiting a histone deacetylase. Nature *391*, 601–605.

Mello, C.C., Kramer, J.M., Stinchcomb, D., and Ambros, V. (1991). Efficient gene transfer in *C. elegans*: extrachromosomal maintenance and integration of transforming sequences. EMBO J. *10*, 3959–3970.

Mittnacht, S., Paterson, H., Olson, M.F., and Marshall, C.J. (1997). Ras signalling is required for inactivation of the tumour suppressor pRb cell-cycle control protein. Curr. Biol. *7*, 219–221.

Muller, H., Moroni, M.C., Vigo, E., Petersen, B.O., Bartek, J., and Helin, K. (1997). Induction of S-phase entry by E2F transcription factors depends on their nuclear localization. Mol. Cell. Biol. *17*, 5508–5520.

Nicolas, E., Morales, V., Magnaghi-Jaulin, L., Harel-Bellan, A., Richard-Foy, H., and Trouche, D. (2000). RbAp48 belongs to the histone deacetylase complex that associates with the retinoblastoma protein. J. Biol. Chem. *275*, 9797–9804.

Nonet, M.L., Staunton, J.E., Kilgard, M.P., Fergestad, T., Hartwieg, E., Horvitz, H.R., Jorgensen, E.M., and Meyer, B.J. (1997). *Caenorhabditis elegans rab-3* mutant synapses exhibit impaired function and are partially depleted of vesicles. J. Neurosci. *17*, 8061–8073.

Page, B.D., Guedes, S., Waring, D., and Priess, J.R. (2001). The *C. elegans* E2F- and DP-related proteins are required for embryonic asymmetry and negatively regulate Ras/Mapk signaling. Mol. Cell *7*, this issue, 451–460.

Peeper, D.S., Upton, T.M., Ladha, M.H., Neuman, E., Zalvide, J., Bernards, R., DeCaprio, J.A., and Ewen, M.E. (1997). Ras signalling linked to the cell-cycle machinery by the retinoblastoma protein. Nature *386*, 177–181.

Potter, C.J., Turenchalk, G.S., and Xu, T. (2000). *Drosophila* in cancer research. An expanding role. Trends Genet. *16*, 33–39.

Reddien, P.W., and Horvitz, H.R. (2000). CED-2/CrkII and CED-10/Rac control phagocytosis and cell migration in *Caenorhabditis elegans*. Nat. Cell Biol. *2*, 131–136.

Rempel, R.E., Saenz-Robles, M.T., Storms, R., Morham, S., Ishida, S., Engel, A., Jakoi, L., Melhem, M.F., Pipas, J.M., Smith, C., and Nevins, J.R. (2000). Loss of E2F4 activity leads to abnormal development of multiple cellular lineages. Mol. Cell *6*, 293–306.

Riddle, D.L., Blumenthal, T., Meyer, B.J., and Priess, J.R. eds. (1997). *C. elegans* II (Cold Spring Harbor, NY: Cold Spring Harbor Laboratory Press).

Sigurdson, D.C., Spanier, G.J., and Herman, R.K. (1984). *Caenorhabditis elegans* deficiency mapping. Genetics *108*, 331–345.

Solari, F., and Ahringer, J. (2000). NURD-complex genes antagonise Ras-induced vulval development in *Caenorhabditis elegans*. Curr. Biol. *10*, 223–226.

Sternberg, P.W., and Horvitz, H.R. (1989). The combined action of two intercellular signaling pathways specifies three cell fates during vulval induction in *C. elegans*. Cell *58*, 679–693.

Sternberg, P.W., and Han, M. (1998). Genetics of RAS signaling in *C. elegans*. Trends Genet. *14*, 466–472.

Sulston, J.E., and Horvitz, H.R. (1977). Post-embryonic cell lineages of the nematode, *Caenorhabditis elegans*. Dev. Biol. *56*, 110–156.

Sulston, J.E., and Horvitz, H.R. (1981). Abnormal cell lineages in mutants of the nematode *Caenorhabditis elegans*. Dev. Biol. *82*, 41–55.

Takahashi, Y., Rayman, J.B., and Dynlacht, B.D. (2000). Analysis of promoter binding by the E2F and pRB families in vivo: distinct E2F proteins mediate activation and repression. Genes Dev. *14*, 804–816.

Tan, P.B., Lackner, M.R., and Kim, S.K. (1998). MAP kinase signaling specificity mediated by the LIN-1 Ets/LIN-31 WH transcription factor complex during *C. elegans* vulval induction. Cell *93*, 569–580.

Thomas, J.H., and Horvitz, H.R. (1999). The *C. elegans* gene *lin-36* acts cell autonomously in the *lin-35* Rb pathway. Development *126*, 3449–3459.

Verona, R., Moberg, K., Estes, S., Starz, M., Vernon, J.P., and Lees, J.A. (1997). E2F activity is regulated by cell cycle-dependent changes in subcellular localization. Mol. Cell. Biol. *17*, 7268–7282.

von Zelewsky, T., Palladino, F., Brunschwig, K., Tobler, H., Hajnal, A., and Muller, F. (2000). The C. elegans Mi-2 chromatin-remodelling proteins function in vulval cell fate determination. Development *127*, 5277–5284.

Walhout, A.J., Sordella, R., Lu, X., Hartley, J.L., Temple, G.F., Brasch, M.A., Thierry-Mieg, N., and Vidal, M. (2000). Protein interaction mapping in *C. elegans* using proteins involved in vulval development. Science *287*, 116–122.

White, J.G., Horvitz, H.R., and Sulston, J.E. (1982). Neurone differentiation in cell lineage mutants of *Caenorhabditis elegans*. Nature *297*, 584–587.

Wu, C.L., Zukerberg, L.R., Ngwu, C., Harlow, E., and Lees, J.A. (1995). In vivo association of E2F and DP family proteins. Mol. Cell. Biol. *15*, 2536–2546.

GenBank Accession Numbers

The GenBank accession numbers for the *dpl-1*, *efl-1*, and *efl-2* genes are AY028165, AY028166, and AY028167, respectively.